

Supplementary Information:

Mass transport and grain growth enable high thermoelectric performance in polycrystalline SnS

Yuxin Li,^a Tao Hong,^b Xiaojun Li,^a Hongxu An,^a Zhanxiang Yin,^{a,c} Mengyue Wu,^d Huiqiang Liang,^e Xiaoqian Wang,^f Lizhong Su,^f Xin Qian,^e Chongjian Zhou,^d Yu Xiao,^c Wenke He,^{a,*} Li-Dong Zhao^{b,g,*}

^aInstitute of Fundamental and Frontier Sciences, University of Electronic Science and Technology of China, Chengdu 611731, China.

^bSchool of Materials Science and Engineering, Beihang University, Beijing 100191, China

^cSchool of Materials and Energy, University of Electronic Science and Technology of China, Chengdu 611731, China.

^dState Key Laboratory of Solidification Processing, and Key Laboratory of Radiation Detection Materials and Devices, Ministry of Industry and Information Technology, Northwestern Polytechnical University, Xi'an 710072, China.

^eCollege of Physical Science and Technology, Hebei University, Baoding 071002, China.

^fSchool of Materials Science and Engineering, Taiyuan University of Science and Technology, Taiyuan 030024, China.

^gState Key Laboratory of Artificial Intelligence for Materials Science, Beihang University, Beijing 100191, China

Correspondence Author: hewenke@uestc.edu.cn; zhaolidong@buaa.edu.cn

Materials and Methods

Synthesis and sintering

High-purity raw materials of Sn granules ($\geq 99.999\%$, Aladdin), S powder ($\geq 99.999\%$, Aladdin) and Na chunk ($\geq 99.999\%$, Aladdin) were weighted in a stoichiometric ratio of $\text{Sn}_{1-x}\text{Na}_x\text{S}$ ($x = 0.003, 0.005, 0.007, 0.01, 0.015, 0.02$), and loaded into carbon-coated quartz tubes. The operation was performed in a glove box with filled nitrogen. The tubes with raw materials were evacuated and flame-sealed under the pressure of $\sim 10^{-3}$ Pa. The outer tubes were used to prevent the samples from oxidation because the inner tubes could break caused by a phase transition (from *Cmcm* to *Pnma*) at high temperature. The samples were slowly heated up to 873 K over 10 h and maintained for 40 h, and then heated up to 1223 K over 6 h and soaked for 10 h, and subsequently furnace-cooled to room temperature. The obtained ingots (~ 10 g) were crushed into powders for following Spark Plasma Sintering (BYT SPS-mini). The sample powder was loaded into a mold with an outer diameter of 50 mm and an inner diameter of 15 mm. All molds were sequentially transferred to the spark plasma sintering system. Under vacuum conditions, an axial pressure of 50 MPa was applied, with a ramp-up time of 11 min, a sintering temperature of 823 K, and a holding time of 10 min. The electrical properties were then tested, as shown in Fig. S1. Subsequently, the $\text{Sn}_{0.99}\text{Na}_{0.01}\text{S}$ samples were weighed according to the specified composition and synthesized following the same procedure, then subjected to spark plasma sintering. Under vacuum conditions, an axial pressure of 50 MPa was applied with varying ramp-up times (9 min, 11 min, 13 min) at 823 K, and a holding time of 10 min. Based on the ramp-up time of 11 min, different holding times (8 min, 12 min, 14 min) were further applied. The final samples were cylindrical with a diameter of 15 mm and a height of 10 mm.

Electrical transport properties

The samples were cut into cuboid-shaped samples with dimensions of $3\text{ mm} \times 3\text{ mm} \times 10\text{ mm}$ for measuring the Seebeck coefficient S and electrical conductivity σ simultaneously, which performed on Cryoall CTA instrument. The samples were

coated with a thin layer of boron nitride to protect the instruments from the possible evaporation of samples. The uncertainty of the Seebeck coefficient and electrical conductivity measurement is within 5%.

Thermal transport properties

The samples were cut into square-like samples with dimensions of 6 mm × 6 mm × (1.0-1.2) mm for thermal transport properties measurement. The thermal conductivity was calculated by the equation of $\kappa = D \cdot \rho \cdot C_p$, where the thermal diffusivity (D) was measured by using the laser flash diffusivity method under LINSEIS LFA 1000, and analyzed using the Cowan model with pulse correction, shown on Fig. S2. The sample density ρ was calculated from the sample mass and dimensions (table S1-S2). The specific heat capacity C_p was calculated using the Debye model. The uncertainty of the thermal conductivity is estimated to be within 8%, considering all the uncertainties from D , C_p and ρ . The combined uncertainty for all measurements involved in the calculation of the final ZT is $\sim 20\%$.

Hall measurements

The samples with dimensions of 8 mm × 8 mm × 0.5 mm was prepared and used for Hall measurements. The Hall coefficient (R_H) was obtained by using the Van der Paw technique under Hall measurement system (Hall-TH6402) equipped with a reversible magnetic field of 1.0 T at room temperature. The measurements at 303 K were performed under argon gas atmosphere to avoid possible oxidation and equipped with a magnetic field of ± 0.9 T. The Hall carrier concentration (n_H) was determined by the equation of $n_H = 1 / (e \cdot R_H)$, and the Hall mobility (μ_H) of carrier was calculated from $\mu_H = \sigma / (e n_H)$, where e is electric charge, and σ is the electrical conductivity.

X-ray diffraction (XRD)

The samples were pulverized with an agate mortar and sifted out through 300 mesh-screen for powder X-ray diffraction measurements (LANScientific-FRINGE CLASS). The powder diffraction patterns were obtained with Cu K α ($\lambda = 1.5418$ Å) radiation in a reflection geometry on a diffractometer operating at 40 kV and 20 mA and equipped

with a position-sensitive detector.

Scanning electron microscopy (SEM)

Scanning electron microscope (SEM, JSM7500, JEOL, Tokyo, Japan) and energy-dispersive spectroscopy (EDS) experiments were carried out. SEM specimens were prepared by conventional methods, including cutting, grinding, dimpling and polishing, etc.

Lorenz number calculations

Considering the complexity and non-parabolicity of valence band in SnS, it is difficult to precisely calculate the Lorenz number (L). An estimation of L also can be made using a single parabolic band (SPB) model with acoustic phonon scattering, resulting in a L with a deviation of less than 10% as compared with a more rigorous single non-parabolic band and multiple bands model calculation. Since the L was used to estimate the lattice thermal conductivity through the Wiedemann-Franz relation, thus, L would not change the total thermal conductivity and final ZT . The Lorenz number is given by formula:

$$L = \left(\frac{k_B}{e} \right)^2 \left(\frac{(r+7/2)F_{r+5/2}(\eta)}{(r+3/2)F_{r+1/2}(\eta)} - \left[\frac{(r+5/2)F_{r+5/2}(\eta)}{(r+3/2)F_{r+1/2}(\eta)} \right]^2 \right) \quad (S1)$$

where k_B is the Boltzmann constant, e is the electric charge, r is the scattering rate, and η refers to the reduced Fermi energy, which can be derived from the measured Seebeck coefficients with consideration of acoustic phonon dominated scattering ($r = -1/2$) via the following equation:

$$S = \frac{k_B}{e} \left[\frac{(r+5/2)F_{r+3/2}(\eta)}{(r+3/2)F_{r+1/2}(\eta)} - \eta \right] \quad (S2)$$

where $F_x(\eta)$ is Fermi integral:

$$F_x(\eta) = \int_0^\infty \frac{\varepsilon^x}{1 + \exp(\varepsilon - \eta)} d\varepsilon \quad (S3)$$

and the density of state (DOS) effective mass ($m^* d$) of hole is determined by Hall carrier concentration (n_H),

$$m_d^* = \frac{1}{k_B T} \left(\frac{2\pi^2 \hbar^3 r_H}{F_{1/2}(\eta)} n_H \right)^{2/3} \quad (S4)$$

where r_H is Hall factor

$$r_H = \frac{3}{4} \frac{F_{1/2}(\eta) F_{-1/2}(\eta)}{[F_0(\eta)]^2} \quad (S5)$$

\hbar is the reduced Planck's constant and T is the temperature.

Debye-Callaway model

Using the Debye-Callaway model, the final temperature (T)-dependent can be expressed as a sum $\kappa_{\text{lat}}(T)$ of the spectral lattice thermal conductivity from different frequencies:

$$\kappa_{\text{lat}} = \int \kappa_s(\omega) d\omega = \frac{1}{3} \int_0^{\omega_a} C_s(\omega) v_g(\omega)^2 \tau_{\text{tot}}(\omega) d\omega \quad (S6)$$

Thus, the $\kappa_s(\omega)$ is determined by the $C_s(\omega)$, the frequency-dependent phonon group velocity $v_g(\omega)$ and total relaxation time $\tau_{\text{tot}}(\omega)$. Generally, as the phonons in optical branches shows low velocity, only the phonons in acoustic branches are considered to calculate the κ_{lat} . Thus, the cut-off frequency for acoustic branches ω_a is given by $\omega_a = (6\pi^2 / V_{\text{cell}})^{1/3}$, $v_s = (6\pi^2 / NV_{\text{av}})^{1/3}$, where N , V_{av} and v_s the atomic numbers in a primitive cell, average atomic volume and sound speed respectively. For simple approximation, the frequency-dependent phonon group velocity $v_g(\omega)$ is set as a constant value v_s , and κ_{lat} is calculated by the following equation (S7):

$$\kappa_{\text{lat}} = \frac{k_B}{2\pi^2 v_s} \left(\frac{k_B}{\hbar} \right)^3 \int_0^{\theta_D/T} \tau_{\text{tot}}(x) \frac{x^4 e^x}{(e^x - 1)^2} dx \quad (S7)$$

The dimensionless variable x in equation (S7) is defined as $x = \hbar\omega/k_B T$, where ω is the phonon frequency. The $\tau_{\text{tot}}(x)$ is the reciprocal sum of the relaxation times from different scattering mechanisms according to the Matthiessen's rule:

$$\tau_{\text{tot}}^{-1} = \tau_U^{-1} + \tau_N^{-1} + \tau_B^{-1} + \tau_{\text{PD}}^{-1} + \dots \quad (S8)$$

Where τ^{-1}_U , τ^{-1}_N , τ^{-1}_B and τ^{-1}_{PD} are the contributions from the Umklapp phonon-phonon scattering, normal phonon-phonon scattering, boundary scattering and point-defect scattering.

The τ -1 U , τ -1 N, τ -1 B and τ -1 PD is calculated from the following equation:

$$\tau_U^{-1} = \frac{2k_B^3 V_{av}^{1/3} \gamma^2 T^3}{(6\pi^2)^{1/3} M v_s^3 \hbar^2} x^2 \exp\left(-\frac{\theta_D}{3T}\right) \quad (S9)$$

$$\tau_N^{-1} = \beta \tau_U^{-1} \quad (S10)$$

$$\tau_B^{-1} = \frac{v_s}{d} \quad (S11)$$

$$\tau_{PD}^{-1} = \frac{V_{av} \Gamma}{4\pi v_s^3} \omega^4 = \frac{V_{av} \Gamma}{4\pi v_s^3} \left(\frac{k_B T}{\hbar}\right)^4 x^4 \quad (S12)$$

Weighted mobility μ_w and details of single parabolic band (SPB) model calculations

the weighted mobility μ_w and the effective mass(m^*) of the carriers are calculated using the experimental S and carrier concentration n_H data measured at 303 K, by the following equations with equation S13 and S14:

$$\mu_w = \frac{3\sigma}{8\pi F_0(\eta)} \left(\frac{\hbar^2}{2m_e k_B T}\right)^{3/2} \quad (S13)$$

$$n = 4\pi \left(\frac{2m^* k_B T}{\hbar^2}\right)^{3/2} F_{1/2}(\eta) \quad (S14)$$

where \hbar is the Plank constant, m^* is the effective mass.

Quality factor (B) calculations

$$B = \left(\frac{k_B}{e}\right)^2 \frac{\sigma_E}{\kappa_{lat}} T \quad (S15)$$

where σ_E is a transport coefficient that can describe the conductive quality in the material at a given η , which is also a function of weighted mobility μ_w mentioned in the above section:

$$\sigma_E = \frac{8\pi e (2m_e k_B T)^{3/2}}{3\hbar^3} \mu_w \quad (S16)$$

In addition, σ_E can be estimated from both Seebeck coefficient S and electrical conductivity σ . Thus, σ_E can also be evaluated by

$$\sigma_E = \sigma \times \exp\left(\frac{|S|}{k_B/e} - 2\right) \quad (\text{S17})$$

On the other hand, the σ as a function of σ_E can be written as

$$\sigma = \sigma_E \times \ln(1 + e^\eta) \quad (\text{S18})$$

Calculations of average ZT (ZT_{ave}) and conversion efficiency (η) calculations

Over a wider temperature range (303-873 K), average ZT value (ZT_{ave}) is given by:

$$ZT_{\text{ave}} = \frac{1}{T_h - T_c} \int_{T_c}^{T_h} ZT dT \quad (\text{S19})$$

where T_h and T_c are the hot and cold side temperature, respectively. In this work, the T_c is 300 K, and T_h is 873 K. Besides, the maximum efficiency (η) over the entire working temperature is determined by the value of ZT_{ave} with T_h and T_c , which can be calculated by:

$$\eta = \frac{T_h - T_c}{T_h} \frac{\sqrt{1 + ZT_{\text{ave}}} - 1}{\sqrt{1 - ZT_{\text{ave}}} + T_c / T_h} \quad (\text{S20})$$

Table S1 Room-temperature density and porosity for different ramp-up time samples, holding time at 10 min.

Samples	9 min	11 min	13 min
Density	4.67	4.76	4.84
Porosity (%)	10.19%	8.46%	6.92%

Table S2 Room-temperature density and porosity for different holding samples, ramp-up time at 11 min.

Samples	8 min	12 min	14 min
Density	4.83	4.76	4.85
Porosity (%)	7.12%	8.46%	6.71%

Table S3 Parameters for the Debye-Callaway model.

Parameter	Symbol	Value	Methods
-----------	--------	-------	---------

Volume per atom for SnS	$V_{av} [\text{\AA}^3]$	24.075	----
Boltzmann constant	$k_B [\text{J/K}]$	1.380649×10^{-23}	----
Grüneisen parameter of SnS	γ	1.72	Ref. 1
Average mass of an atom of SnS	$M [\text{kg}]$	1.2523×10^{-24}	Calculate
Average sound velocity of SnS	$v [\text{m/s}]$	2424	Ref. 2
Debye temperature of SnS	θ_D	270	Ref. 3
Reduced Planck constant	$\hbar [\text{J}\cdot\text{s}]$	$1.05457266 \times 10^{-34}$	----
Ratio of Normal phonon scattering to Umklapp scattering	β	20	Ref. 4
Average grain size	$d [\mu\text{m}]$	15	SEM
Disorder scattering parameter	Γ	0.11806	Calculate

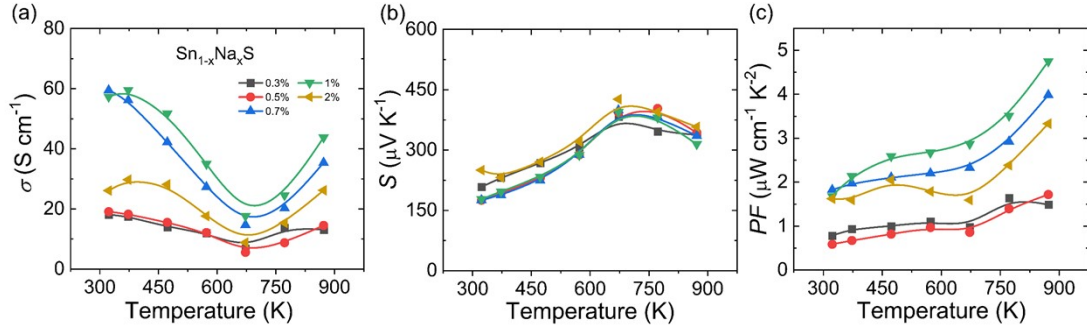


Fig. S1 Electrical properties of Sn_{1-x}Na_xS (x = 0.003, 0.005, 0.007, 0.01, 0.02). (a) Electrical conductivity. (b) Seebeck coefficient. (c) Power factor.

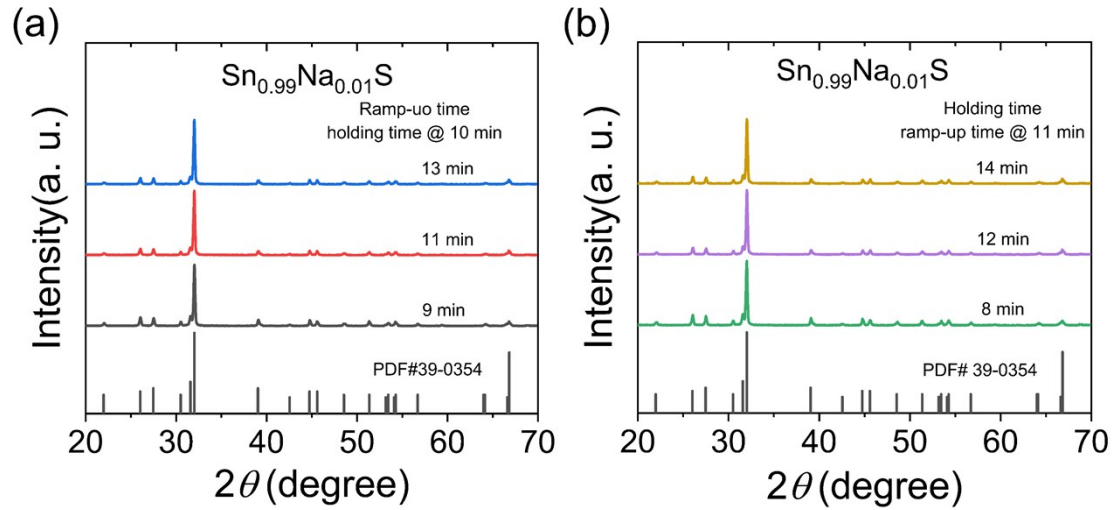


Fig. S2 Power X-ray diffraction of $\text{Sn}_{0.99}\text{Na}_{0.01}\text{S}$ with different (a) ramp-up time and (b) holding time.

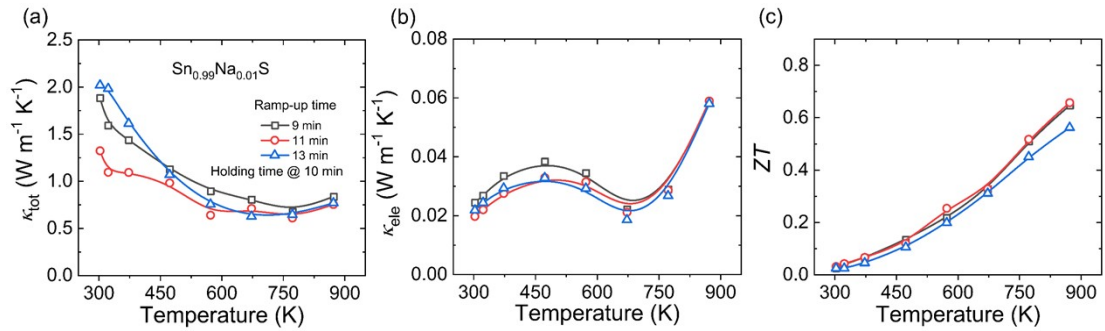


Fig. S3 (a) Total thermal conductivity, (b) Electronic thermal conductivity and (b) ZT of $\text{Sn}_{0.99}\text{Na}_{0.01}\text{S}$ with different ramp-up time.

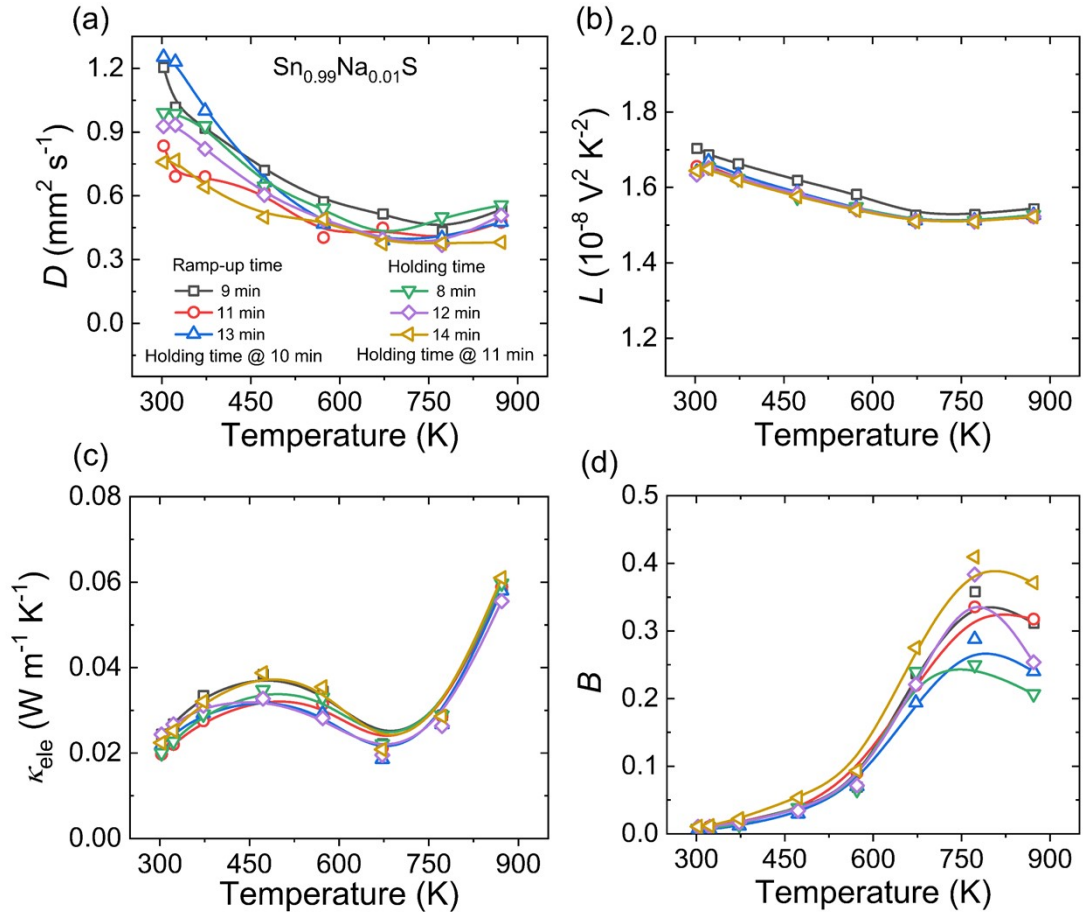


Fig. S4 Thermoelectric properties of $\text{Sn}_{0.99}\text{Na}_{0.01}\text{S}$ with different ramp-up and holding time. (a) Thermal diffusivity. (b) Lorentz constant. (c) Electrical thermal conductivity. (d) Quality factor.

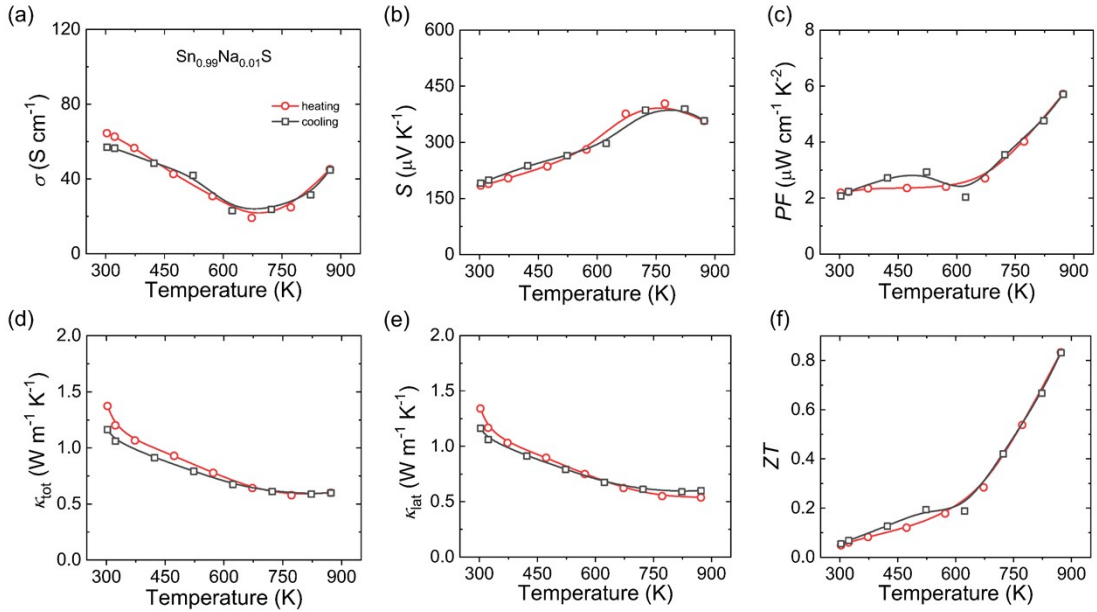


Fig. S5 The thermoelectric performance of the optimal sample under thermal cycling conditions. (a) Electrical conductivity. (b) Seebeck. (c) Power factor. (d) Total thermal conductivity. (e) Lattice thermal conductivity. (f) ZT .

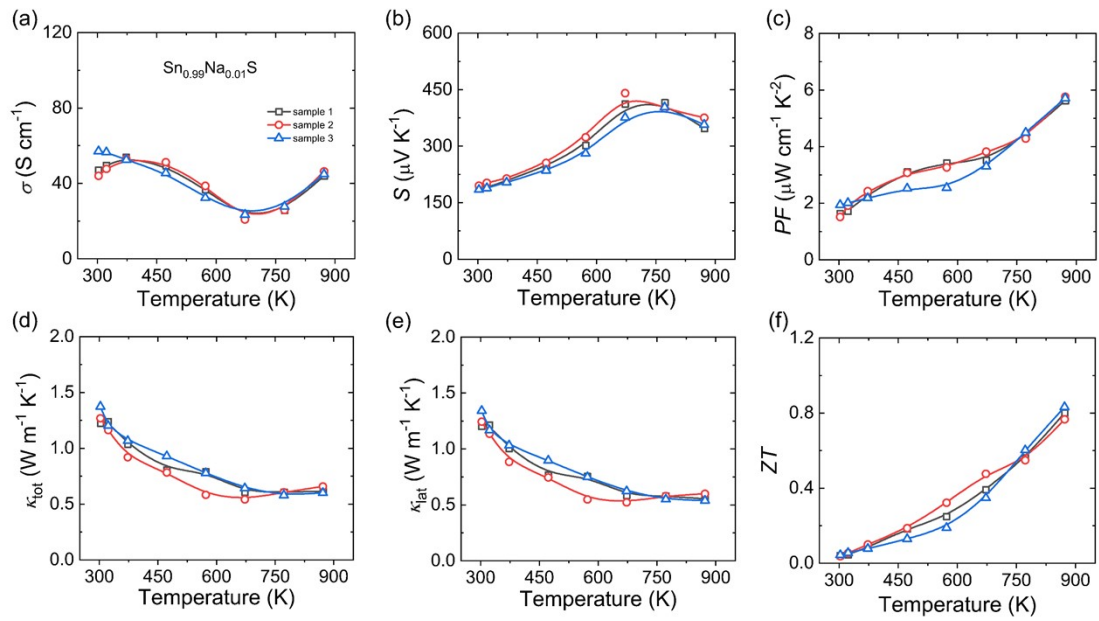


Fig. S6 Reproducible thermoelectric performance of the optimized sample. (a) Electrical conductivity. (b) Seebeck. (c) Power factor. (d) Total thermal conductivity. (e) Lattice thermal conductivity. (f) ZT .

Reference

1. R. Q. Guo, X. J. Wang, Y. D. Kuang and B. Huang, *Phys. Rev. B*, 2015, **92**, 115202
2. B. Q. Zhou, S. Li, W. Li, J. Li, X. Y. Zhang, S. Lin, Z. Chen and Y. Pei, *ACS Appl. Mater. Interfaces*, 2017, **9**, 34033-34041.
3. Y. M. Han, J. Zhao, M. Zhou, X.-X. Jiang, H.-Q. Leng and L.-F. Li, *J. Mater. Chem. A*, 2015, **3**, 4555-4559.
4. Asfandiyar, B. W. Cai, L. D. Zhao and J. F. Li, *J. Materiomics*, 2020, **6**, 77-85.